07(XV)-78 **Topology Independent Model for Medical Robotic Simulation**

C. Chui[a], I. Sakuma[a]

[a] *Department of Mechanical Engineering, National University of Singapore, Singapore*

[b] *Department of Precision Engineering, The University of Tokyo, Tokyo, Japan*

Abstract: The field of medical robotic is relatively new, and computer aided surgical system with robot for treatment delivery has not been fully exploited. An approach in advancing this field is via a more efficient preparation of the robotic surgical intervention using computer simulation. In the virtual medical robotic system that we are developing for fluoroscopic image guided liver-needle insertion and ablation, C-Arm as well as one or more needle insertion robots are represented as independent robotic models in one work cell. Unlike typical industrial robot, medical robot is operating on an unstructured clinical environment with many variations. In order to provide the computational power required for medical robotic simulation, we are exploring parallel computing using a microcomputer system with multiple core processors. Instead of relying on the task scheduler based upon load balancing, we investigated LogP which is a theoretical model that does not consider the topology of the communication network. The network is represented using parameters that account for limited bandwidth into and out of the processor, latency and overhead. We demonstrated that parallel algorithms can be derived and evaluated using this model.

Key words: Medical robot, Surgical simulation, Parallel processing, Theory of Computing

1. Introduction

By extending human surgeon's ability to plan and carry out surgical interventions more accurately and less invasively, computer aided surgical system including medical robotic, can greatly reduce costs, improve clinical outcomes, and improve the efficiency of health care delivery. The field of medical robotic is relatively new, and computer aided surgical system with robot for treatment delivery is far from being full exploited. A solution to remedy this discrepancy is through a more efficient preparation of the intervention via computer simulation. However, computer simulation of medical robotic is still very much in its infancy.

Medical robotic development systems including graphical simulation are of considerable interest [1], for several reasons. Such systems permit planning and evaluation of the robot and/or related surgical equipment before they are used in the surgery. They permit the programming of robot away from the clinical environment in which it must operate. The risk of damage is reduced if it is possible to visually inspect the execution of the task on a graphic screen before it is executed clinically. Nevertheless, this is a complex and computationally intensive process, and unlike industrial robotic system, we are working on an unstructured clinical environment with many variations that will demand frequent parameter changes and interactive simulation.

In our virtual medical robotic systems for fluoroscopic image guided needle insertion, the robot and C-arm are represented as independent robotic models in one work cell. An objective of the simulation is to derive with our conceptual robot the optimal needle placement and insertion with unobstructed view from C-Arm and minimal X-ray dosage.

Despite the recent advancement of parallel computing hardware such as workstation cluster, and recently, microcomputer system with multiple core processors, it remains an issue on how to fully utilize this computing hardware to deliver optimal performance. In this paper, we describe our investigation on two theoretical models for cluster and multicore computing respectively for medical robotic simulation.

2. The LogP Model

In LogP model [2, 3], communication between processors is represented by a set of parameters, and through a broadcasting media. The LogP model is originally targeted as a model for multiprocessor systems, and is independent of the communication network topology. We want to use the LogP model to design and evaluate parallel/distributed algorithms for real time simulation of robot operations.

The LogP model we use contains the following components:

- P processors that run asynchronously and independently.
- An interconnection network whose topology is of no concern to us, except that we know:
  - g, a single parameter that accounts for limited bandwidth into and out of the processor. It is the rate at which a processor can send words into the network when it is ready to do so.
  - L is the latency.
  - o is the overhead, accounting for all other time in the execution of the remote instruction during which the processor is unavailable for computing.

g approximates $(1/B)$ where B is the bandwidth of the entire network. If an instruction is executed at a source at time t, the solution is not available at the destination until

$t + L$. The model is useful when it can be used to design and devaluate a large class of algorithms related to robotic simulation.

3. Performance Evaluation using LogP Model

We will start by proving the desired performance of this model using one-to-all broadcasting in Lemma 1, and all-to-all broadcasting in Lemma 2. One-to-all and all-to-all broadcasting are fundamental operations that appear many time as subtasks in medical robotic simulation. Note that g is the most important factor considered in our theoretical analysis, and to transmit n elements from one processor to another processor requires $O(ng)$ time.

Lemma 1: One-to-All Broadcast

If one processor needs to send n elements to all other P-1 processors, it can be done in $O(ng\log P)$ time.

Suppose that there are P processors. Any one processor p wants to send a vector b of n elements to all other processors as in procedure One-to-All Broadcast. In this procedure, we may conceptually regard the execution as a binary tree, and the execution starts in top-down mode.

For example, if processor P_0 is to broadcast n elements to all other processors, it will send these elements to processors P_1 and P_2. They will then transmit these elements to P_3, P_4 and P_5, P_6 respectively in a concurrent manner. This process repeats until all processors receive the elements. The number of recursion equals to the depth of the tree. The height of the tree is $O(\log P)$. It is clear that the time complexity is $O(ng \log P)$.

Note that we can improve the $O(ng \log P)$ time complexity to $O(ng + g\log P)$ by pipelining the transmissions of the n elements.

Lemma 2: All-to-All Broadcast

If all processors need to send n elements to all other processors, and there are P processors, it can be done in $O(ng P)$ time with no conflict.

Suppose that there are P processors, and each processor wants to send a vector b to all other processors. It is obvious that this will require $O(ng P \log P)$ time if we will to use procedure One-to-All Broadcast P times to accomplish the task. A more natural way is given in procedure All-to-All Broadcast. It is clear that there is no conflict in communication and $O(ng P)$ time is required for this procedure.

Lemma 1 and Lemma 2 provide the theoretical basis to derive and evaluate theoretical optimal algorithms for other parallel scalar and matrix operations

```
Procedure One-to-All Broadcast {
   If all processors receive b then stop
   Else recursively transmit to the next two
   processors that do not yet receive b
}
Procedure All-to-All Broadcast {
   For k=1 to P-1
      For each processor p do in parallel
         Send b to processor (p+k) mod P
         Receive b from processor (p-k) mod
         P
}
```

Fig.1 Broadcast algorithms

4. Discussion and Conclusion

It is difficult is achieve optimal performance on parallel/distributed computing system using typical tasks scheduling methods based on load balancing. In this paper, we described our investigation on the application of LogP model which is a topology independent model, in derivation and evaluation of parallel algorithms for medical robotic simulation. Our work on the LogP model focuses on efficient computation. This is different from previous works that concentrated primarily on communication.

Reference

1) Falk V, F Mourgues et al (2005). Cardio navigation: planning, simulation, and augmented reality in robotic assisted endoscopic bypass grafting, Ann Thorac Surg 79(6): 2040-2047
2) Culler D, R Karp et al (1993). LogP: towards a realistic model of parallel computation, Principles Practice of Parallel Programming, pp. 1-12.
3) Chui C, S Jain et al (1994). Research activities in accelerated computing and theory program (ACT program), J High Performance Computing 1(1): 50-57.

Paper:

Development of an Intraoperative Information Integration System and Implementation for Neurosurgery

Eisuke Aoki*, Masafumi Noguchi*, Jae-Sung Hong**, Etsuko Kobayashi***, Ryoichi Nakamura****, Takashi Maruyama****, Yoshihiro Muragaki****, Hiroshi Iseki****, and Ichiro Sakuma***

*Graduate School of Frontier Sciences, The University of Tokyo
7-3-1 Hongo, Bunkyo-ku, Tokyo 113-8656, Japan
E-mail: aoki@miki.pe.u-tokyo.ac.jp
**Department of Nanobiomedicine, Faculty of Medical Sciences, Kyushu University
3-1-1 Maidashi, Higashi-ku, Fukuoka 812-8582, Japan
***Department of Precision Engineering, School of Engineering, The University of Tokyo
7-3-1 Hongo, Bunkyo-ku, Tokyo 113-8656, Japan
****Institute of Advanced Biomedical Engineering and Science, Tokyo Women's Medical University
8-1 Kawada-cho, Shinjuku-ku, Tokyo 162-8666, Japan
[Received October 18, 2006; accepted March 24, 2007]

Complete resection of glioma is required to obtain a satisfactory outcome in neurosurgical treatment. It is difficult for neurosurgeons to identify the boundary between glioma and normal tissue using the naked eye alone, so surgical assistance systems such as surgical navigation systems for the detection of brain tumor have been used in clinical operations. Intraoperative information obtained from intraoperative biomedical measurement systems must be integrated to detect brain tumors more accurately. In this research, we developed an intraoperative information integration platform using middleware that has global positioning and global time management capabilities. To evaluate the platform, we developed an integrated platform consisting of devices and systems for neurosurgery. Through experiments, we confirmed the basic performance and effectiveness of our platform in a simulated clinical environment.

Keywords: system integration, neurosurgery, distributed system, 5-aminolevulinic acid, navigation system

1. Background

In recent years, a number of research laboratories are expected to develop devices and systems supporting minimally invasive surgery and its effects [1–3]. In order to perform more effective surgical operations, appropriate computer-assisted surgery is needed based on the required function, so an integrated system is needed that supports surgeons in an environment in which surgical devices are integrated.

In order to integrate a system, communication software is needed for connecting computers that control and manage multiple surgical devices, as is software to mutually integrate individual systems. If the development environments of individual systems differ, it takes much time and cost to develop such software.

As a solution, we have developed an intraoperative information integration system utilizing distributed object technology (middleware) [4]. When using distributed object technology, differences in operating systems (OSs) and hardware are made transparent and the development of application software operating under different platforms is facilitated. Parallel processing to distribute a load over multiple computers then becomes possible [5].

For these reasons, computer-assisted surgical systems using distributed object technology are being widely developed. Knappe et al., for example, developed a navigation robot reusing an existing system having a different development environment and specifications to reduce development time and cost [6]. Schorr et al. distributed the calculation load of image processing, which takes time in navigation processing, by using multiple PCs to develop a navigation system enabling real-time information presentation [7]. For improving performance by reducing development time and cost and distributing the load of calculation processing, computer-assisted surgical systems have thus been developed using distributed object technology [6–8].

When considering the construction of an integrated computer-assisted surgery environment, a problem arises in a distributed system using multiple computers because individual computers do not always indicate the same time, and the positional information of computer-assisted surgical devices may not be mutually associated correctly. To solve this problem, we must standardize time information, including mutual time synchronization of subsystem components and the integration of positional information. The integration of positional information has been fully discussed in an integrated system using multiple surgical devices [6–8]. Time has not, however, been sufficiently

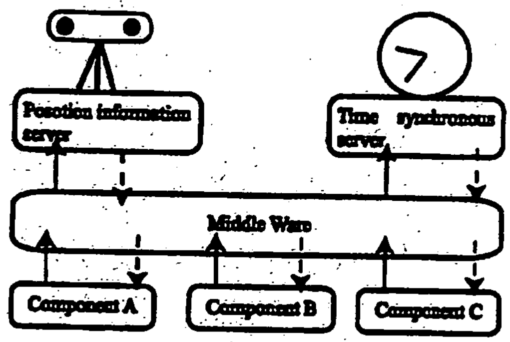

Fig. 1. System overview: system integration platform for surgery assisting system is consisted of global position server, global time server and components.

clarified and standardized in conventional studies.

In dealing with biological information, the positional information of organs varies from hour to hour as typified by bodily movement. To integrate biological information from multiple measuring instruments, the timing between measuring instruments must be standardized highly precisely.

Based on the above, we use not only distributed object technology and but also develop an integrated platform focusing on the integration of positioning and timing. Our discussions here focus on the highly precise standardization of timing, which is important for performing advanced computer-assisted surgery. We then apply the integrated platform to an actual surgery-assisted system for neurosurgery and verify its effectiveness through an evaluation experiment, as reported in the sections that follow.

2. Methods

2.1. System Configuration

We focus on three functions for realizing an integrated platform for a computer-assisted surgical system:

1. The integration of surgical devices having different development languages and environments.
2. The integration of positioning information.
3. The standardization of timing information.

In order to realize the integration of surgical devices having different development languages and environments, we use distributed object technology. In order to realize the integration of positioning information and the standardization of timing information, we established a time-synchronous server for providing standardized timing and positioning information servers for providing integrated positioning information in the integrated platform. We also provide communication software components for connecting components of surgical systems with the present platform (Fig. 1).

Table 1. Classification of middleware.

	OS independent	Language independent	Real Time
NDDS	○	○	◎
JAVA RMI	◎	×	△
COM	×	○	△
CORBA	○	◎	△

2.2. Use of Distributed Object Technology

Widely used middleware includes JAVA Remote Message Invocation (JAVA RMI), Distributed Component Object Model (DCOM), Common Object Request Broker Architecture (CORBA), and the Network Data Distribution Service (NDDS) (Table 1). CORBA is actively studied and developed, having many supported development environments and programming languages [5–10].

Communication in CORBA is based on TCP/IP. In TCP, data lost during communication is retransmitted (Retransmission Control). Communication is controlled to adjust the amount of data based on available communication conditions (Congestion Control). TCP retransmission and congestion control is effective when data is transferred securely to a destination, but communication time cannot be estimated because data retransmission and the transmission amount are adjusted.

Unlike TCP, UDP does not perform retransmission control if communication information is lost during communication. While transmission of information is not ensured, communication having an immediate response is realized. In the control of mechatronics equipment, which requires strict real-time performance such as high-speed sampling, communication control having an immediate response rather than data reliability is needed. In controlling a computer-assisted surgery robot, UDP communication is preferable. By adding functions of retransmission and congestion control to the communication based on UDP, reliable communication such as TCP can be realized.

In the present study, we used NDDS (WaveWorks(R), RTI, USA), which is a type of distributed object technology based on UDP/IP [11]. NDDS uses a Real Time Subscribe (RTPS) communication model, which does not require an intermediation server or irrelevant request message.

2.3. Integration of Standard Positioning Information by Positioning Information Server

In managing systems by using an integrated coordinates, setting position of individual equipment are measured by using an external sensor, which we also use, and based on this, information from individual equipment is integrated into the standard coordinates.

External sensors include mechanical sensors measuring the location of the tip of a multijointed arm by an encoder detecting the angle of each joint, magnetic sensors detecting positioning by generating a magnetic field and measuring the intensity of the magnetic field by a magnetic field sensor attached to a probe, and optical sensors detecting positioning by using a CCD camera to capture the light reflected from an exclusive reflective marker attached to a probe.

The area measured by a mechanical sensor is limited to the driving range of a robot's mechanical arm. Magnetic sensor measurement error occurs due to magnetic materials around the target to be measured, and this restricts its use, depending on the surgical environment. Optical sensors involve the problem of blocking by obstacles, but enabling unrestricted measurement and comparatively higher measurement accuracy.

Based on the above, and considering reliability, expansion ease, precision, and the environment used in measurement, we used an optical three-dimensional positioning measurement device (POLARIS®, Northern Digital Inc. Canada) that uses reflective markers. Its sampling speed is approximately 60 Hz and root-mean-square (RMS) precision is 0.35 mm in positioning measurement of reflective markers. The positioning information server measures positioning information of the surgical device set up in the operating room and integrates coordinates with an optical position measurement device providing the standard coordinates.

2.4. Standardization of Timing Information by Time Synchronization Server

2.4.1. Requirement Specifications

OS generally standardize integrated time systems using network time protocols (NTP) via Internet connection. The NTP acquires correct time using the Global Positioning System(GPS) to adjust internal computer clocks based on world standard time.

Information must be managed highly confidentially when treatment information including private patient information used in surgery, which is why data is not usually transmitted or received via the Internet. Configuring practical computer-assisted surgery requires an integrated platform, regardless of the system environment, where information among computers in the operating room is limited to LANs (LANs). For this we use a time synchronization server generating a standard LAN time that differs from actual time.

To realize integrated computer-assisted surgery, information from multiple measuring instruments must be integrated so that subsystem time is synchronized with current standard time. In intraoperative logging recording surgery information, massive bleeding is a serious problem, before and after which information on equipment and operation is recorded as a time-series, allowing a lag from actual time.

The time synchronization server issuing standard time in an integrated system operates continuously. If a failure occurs in a single time synchronization server, standard time is lost, so the time synchronization server is rebooted, which loses consistency with time in intraoperative information recorded previously. Standard time in the integrated system must therefore be maintained regardless of problems in the time synchronization server.

When dealing with biological information, precise treatment information cannot be obtained if a time lag exists among measuring instruments. Tokuda et al. measured hepatic motion via breathing to show that a positioning variation of 50-60 mm is created at intervals of 7-8 seconds [12]. When position accuracy required for computer-assisted surgery is 1 mm, to obtain accurate treatment information for an ever-changing organism, time must be standardized to within 100 ms. To do so while considering the communication time lag, time resolution, and lag of measuring instruments and the time lag of the drive used together, it must be as fast as possible, so we set it to 30 ms. Under the system environment limited to the LAN, (a) time is precisely standardized at 30 ms and (b) the time synchronization server is fault-tolerant ensuring standard time continuity.

2.4.2. Time Synchronization Algorithm

A time synchronization server having high-precision standardization of time and fault-tolerant performance realizes functions according to the following flow:

(a) One of the subsystems is started as a time server.

(b) When a new system is added, time is synchronized with the present time server.

(c) If a failure occurs in the present time server, another subsystem becomes the time server to maintain the continuity of time management in the system.

2.4.3. High-Precision Standardization of Time

To realize high-precision standardization of time, it is necessary to consider two things:

- The lag created by the progress of the clock of each computer.
- The lag created by the communication time delay at the time of synchronization.

Regarding the lag created by the progress of the clock of each computer, progress can be adjusted by increasing the frequency of updating with the time synchronization server. The lag created by the communication time delay at the time of synchronization denotes the precision (hereafter, time synchronization precision) when synchronizing with the time synchronization server and the corrective effect of lags due to individual computer clocks depends on the time-synchronous precision of lags due to the communication time delay at time synchronization. Accordingly, to perform high-precision time synchronization, it is desirable to solve the problem of communication delay time.

In CORBA, TimeService is prepared as a service for synchronizing time [13]. It only obtains time issued by the TimeService, however, and communication delay time is not considered. In a one-to-one client-server system configured in a LAN environment, Dalton et al. show that there is an unsteadiness of communication time of from several ms to several tens of ms [14]. Schorr et al. show that a maximum 40 ms delay is created in communication processing time [7]. Depending on the communication environment to be used, reliable time synchronization is difficult to achieve when communication delay time is not considered.

In the present article, we employ a time-synchronous algorithm considering the communication time based on a formula (1) proposed by Cristian et al. [15]. In Cristian's algorithm (formula (1)), loopback time $(T2 - T1 - S)$ from the client to the server is measured, half of the loopback time $(T2 - T1 - S)$ is added to the time (G_{server}) sent from the server, and the time-synchronous time (G_{client}) is obtained.

$$G_{client} = G_{server} + \frac{(T2 - T1 - S)}{2} \quad \ldots\ldots \quad (1)$$

G_{client}: time-synchronous time
G_{server}: time of time-synchronous server
$T2$: time when data is received from server
$T1$: time when data is sent to server
S: processing time at server

The problem with this method is that half of the loopback time cannot strictly be said to be communication time. The factor is cited that the round-trip communication time of the network is not always the same. When the loopback time is short enough, the round-trip time lag is small and can almost be neglected. That is, in the case of employing Cristian's method, time-synchronous precision is improved by synchronizing time when the loopback time is short, but communication conditions of the network are not fixed, therefore the decision criterion of whether loopback time is short or not should be decided according to circumstances.

In summary, in order to realize high-precision time synchronization, time synchronization is performed according to flows (a) to (c) as follows:

(a) Measure the loopback with the time server 100 times to calculate average (t) of the loopback time and its variation (σ).
(b) From a statistical value obtained from (a), communication time is estimated to be $(t - \sigma)$ when the network is relatively idle.
(c) When communication time is equal to or smaller than assumed value $(t - \sigma)$, synchronize time by adding communication time.

We adopt a policy in which, after time synchronization, if the consistency of time cannot be maintained among subsystems, for example, when transmitted time precedes reception time, synchronization is performed again.

2.4.4. Time Synchronization Server Having Fault Tolerance

The present system is designed to have failure tolerance using the following algorithm (Fig. 2):

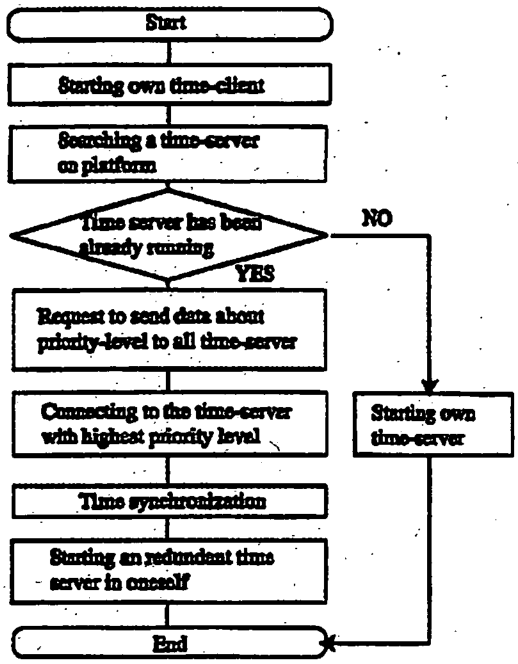

Fig. 2. Flow chart of fault tolerant time synchronization algorithm.

- All systems have time synchronization servers and clients communicating with the server to be connected to the platform.
- If no time synchronization server is present, the system itself becomes the time synchronization server.
- When a time synchronization server is present, the system becomes a client to be synchronized with the server. When multiple time synchronization servers are present, time is synchronized with the server having the highest priority.
- After completing time synchronization, the connected system drives the prioritized time synchronization server having priority. Clock performance is measured in advance and priority is allocated based on performance.

Thanks to such algorithms, even if the currently operating time synchronization server stops functioning, the server with second priority (the time synchronization server in operation having the highest priority) starts. The time consistency of the subsystem is maintained by the redundant time synchronization server (Fig. 3).

As mentioned before, actual time is not so important that prioritization based on the clock accuracy of the computer does not have an important meaning. Changing to a time synchronization server having a largely different clock performance, however, is not desirable because there is the possibility that a time lag may be created in the integrated system. Clock performance is therefore measured in advance and priority is allocated in turn based on performance.

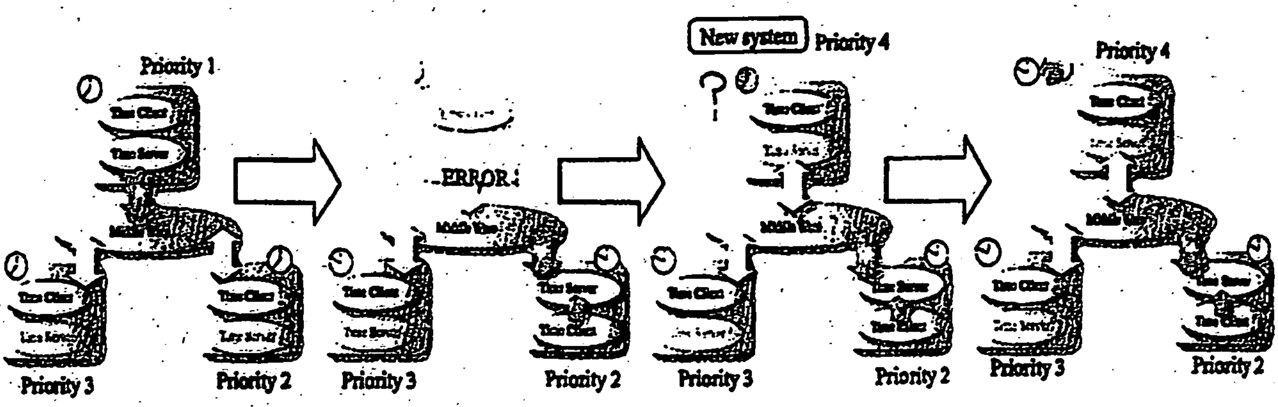

Fig. 3. Fault tolerant algorithm of the whole system; priority 1 > 2 > 3 > 4.

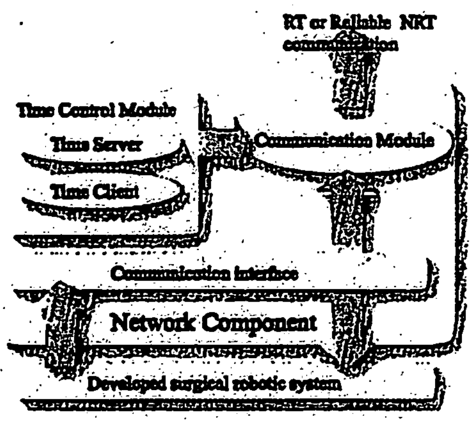

Fig. 4. Overview of network component.

2.5. Communication Component Module

To realize a time synchronization server having time consistency and fault-tolerant performance, as mentioned above, software to perform the function is required to be implemented for each component connected to the platform. It is problematic, however, in view of development efficiency, to have separate correspondence to software implementation operation for each system, we developed a communication component (class library) having the time synchronization function above (Fig. 4).

Depending on the computer-assisted surgical system to be used, the requirement for communication may differ. When controlling a computer-assisted surgery robot, for example, communication having an immediate response is required. When recording intraoperative information for which security is important, an immediate response is not necessary; instead, ordered and secure transmission and reception of information is required.

We therefore implement two types of communication modules into the communication component to enable communication to be selected based on the system: a RealTime communication module (RT communication) to realize communication having an immediate response based on UDP/IP and a Reliable communication module (Reliable communication) to make data transmission and reception secure through the functions of retransmission control and congestion control with no real-time performance. When information to be transmitted is being transferred from a corresponding surgical device, the communication component starts a thread performing time synchronization in the background to synchronize time with the time synchronization server in the network. When data is transferred through a communication interface from the corresponding surgical device, integrated time information is added to the data as a time stamp and data is transmitted and received by a selected communication module (RT communication or Reliable communication). Regarding such a time synchronization function and communication control of the network, all processing is performed in the background.

The above points ensure data transfer between platforms for users without having to change the control software of the existing surgical device, etc., simply by deciding data interface transmission to and reception from the network.

3. Application to Neurosurgical Surgery-Assisted System

We have associated the fluorescence intensity and spectrum information obtained from 5-aminolevulinic acid (5ALA) induced protoporphyrin IX (Pp9) fluorescence with cancer malignancy as a neurosurgical surgery-assisted system to develop a cancer detection system for quantitative diagnosis [1,2]. Even if a cancerous area is identified by this cancer detection system, it is difficult to remove cancer if it is close to an important functional region but the positional relationship of a patient's motor language area to the motor area (functional information) is not sufficiently clear.

In surgery using a navigation system based on preoperative diagnostic information, the location of the unclear cancer boundary (anatomical information) and the cerebral function region (functional information) of motor language area and motor area, etc., is presented to the surgeon as objective three-dimensional image information. More effective surgical navigation is realized with histological information such as cancer malignancy detected by Pp9 fluorescence measurement being presented to the surgeon together with cerebral functional and anatomic information by this navigation system.

We therefore applied the position server, time server, and communication component we developed to a surgery-assisted system for neurosurgery. We configured an integrated navigation system that collects and integrates information from multiple intraoperative measuring instruments to display on a navigation screen. Functions of the integrated system are realized in the following flow:

(a) Standardization of time between subsystems.

(b) Integration of coordinates to unify positioning-information by using a positioning-information server.

(c) Collection of multiple intraoperative information associated with positioning.

(d) Integration of information from time information added simultaneously to intraoperative information.

(e) Integration of preoperative and intraoperative information obtained from a diagnostic imaging system.

(f) Extraction of integrated information based on surgical conditions to display as intuitive information on the navigation screen to the surgeon.

The integrated system consists of the following five computer-assisted surgical systems.

3.1. Cancer Detection System by Intraoperative Cerebral Cancer Fluorescence Diagnosis Using 5ALA-Induced PpIX

5-ALA-induced fluorescent material Pp9 in cancer tissue is excited locally using a 405 nm excitation laser to detect the red fluorescence of an emission wavelength peak of 635 nm using a detector made of optical fiber. The spatial resolution of the detector is 0.6 mm. Detected fluorescence is spectrally analyzed by a spectral photometer, then histological information on the malignancy and type of cancer is obtained as quantitative information from the intensity and spectrum of the fluorescence signal (Fig. 5(b)) [1].

3.2. Autofocusing Robot

It is essential to stable fluorescence measurement to keep sufficient distance between the fluorescence detector and the subject being measured. This requires an automated positioning control function that unfailingly makes the operating distance between the fluorescence detector and the object surface coincide. In the present study, we placed a fluorescence probe on a surgical microscope (Mitaka Kohki Co., Ltd.) equipped with an automated positioning control function that maintains a fixed distance between the microscope and the object being measured

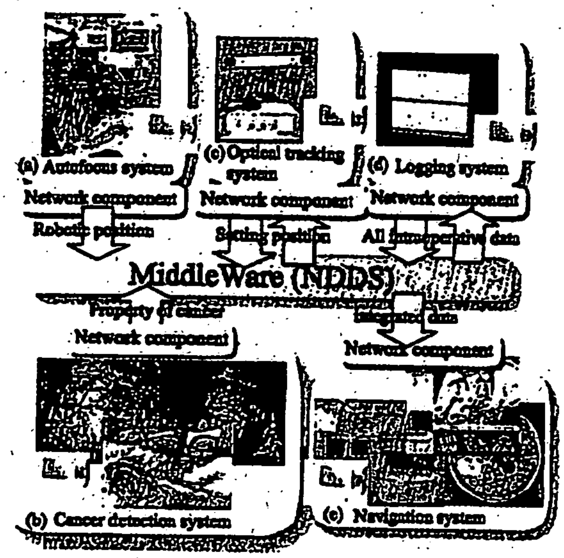

Fig. 5. Integrated neurosurgical robotic platform using NDDS.

(Fig. 5(a)). By combining a two-axis robot stage (scanning robot), positioning measurement becomes possible while the robot drive is scanning the brain surface.

In the present system, we measure positioning using a confocal optical system in a confocal laser microscope. Positioning measurement, which distinguishes top and bottom of an object using a principle similar to the optical pickup of CDs, becomes possible by concentrating a guide laser with a wavelength of 670 nm on the surface of an object and using a two-fraction diode in place of a pin hole in the detector [2]. When the object is a metal with stain finished surface, it is possible to ensure positioning with an accuracy of 2.0 μm.

3.3. Navigation System

Three-dimensional image information is prepared based on preoperative diagnosis information such as Magnetic Resonance Imaging (MRI), and spatial positioning of the object being treated is intuitively shown to the surgeon. As the navigation system, we used a system developed by the Kyushu University Center for the Integration of Advanced Medicine and Innovative Technology that is based on a 3D slicer [16], which is free software. The navigation system [3] displays three-dimensional imaging information, including the boundary between cancerous and normal tissue and functional information on the brain, etc., to the surgeon qualitatively and in real time (Fig. 5(e)).

3.4. Positioning-Information Server (Section 2.3)

As mentioned in Section 2.3, by using an optical position measurement device as the position measurement device, three-dimensional positioning-information of the surgical device established in the operating room is measured and coordination integration is performed (Fig. 5(c)).

3.5. Intraoperative Logging System

An intraoperative logging system monitors and records intraoperative logging information such as the condition and function of measuring instruments during surgery. By tracing and analyzing logging information, it is determined whether the surgical robot and measuring instruments are functioning without problems, and if problems occur, the cause of the error is checked (Fig. 5(d)).

4. Evaluation Experiments

We confirmed high-precision time standardization of 30 ms and the fault-tolerant performance of the time-synchronous server through evaluation experiments in a laboratory environment. We also confirmed functions of the entire integrated system through an *in vivo* experiment simulating clinical use.

4.1. Evaluation of Integrity of Integrated Time

In cerebral nerve surgery, some surgeries take as long as 10 hours or more to remove malignant cancer.

Assuming that the computer-assisted surgical system is applied practically in clinical use, we evaluated the integrity of time information with and without time-synchronization during 12 hours of continuous system operation.

4.1.1. Experimental Methods

For experiments, we prepared intraoperative logging (OS: Redhat 9.0, CPU: 3.2 GHz, Memory: 1024 MB) in which the time-synchronous server is operated, measurement system A (OS: Windows XP, CPU: 3.04 GHz, Memory: 1024 MB) using Windows, and measurement system B (Redhat 9.0, CPU: 3.04 GHz, Memory: 1024 MB) using Linux. After ensuring time synchronization once, the current time of each measurement system is transmitted to intraoperative logging at intervals of 20 ms. The time of each system received in a 20 ms cycle is recorded along with the time of the time-synchronous server at intervals of 1 s.

Under such circumstances, we evaluated time lag with the time-synchronous server with the system as is for 12 hours when (a) time is synchronized every 20 minutes and (b) time synchronization is not done and left as is. The time lag evaluated is the difference between the time of each measurement system, which intra-operative logging receives, and the time when the time-synchronous server is recorded. Since measurement and intra-operative logging ensure asynchronous communication, 20 ms becomes the time resolution, which is evaluated and equivalent to the transmission period. Communication is in a 100 Mbase-T LAN environment.

4.1.2. Results of Experiments

Table 2 shows time lag with the time-synchronous server using the elapse of one hour as a criterion when time synchronization is not done and when the time is synchronized every 20 minutes for Windows and Linux. When time is not synchronized, an increase in the time lag is seen over time. The time until 30 ms, a required specification we set, is exceeded takes 8 minutes for Windows and 26 minutes for Linux.

Table 2. Time lag with and without a timeserver.

Elapsed time [hour]	Windows without timeserver [msec]	Windows with timeserver [msec]	Linux without timeserver [msec]	Linux with timeserver [msec]
1	265	97	69	10
2	610	41	130	11
3	1016	41	184	11
4	1392	41	232	10
5	1848	42	289	11
6	2265	42	341	11
7	2265	43	341	11
8	3093	43	445	10
9	3502	43	498	10
10	3915	44	550	11
11	4330	43	604	10
12	4743	28	657	11

When time is synchronized every 20 minutes, no increase in time lag was seen over for either Windows or Linux. More clock fluctuation was seen for Windows than Linux, i.e., when the time lag is 10-11 ms for Linux, it is 28-97 ms for Windows. In the experiment below, time-synchronous server priority is preferentially given to Linux due to its smaller clock fluctuation. For the same OS, priority is given to the computer having better performance. To realize time synchronization of 30 ms, time synchronization frequency is given a margin such as every 20 minutes for Linux and every 5 minutes for Windows.

4.2. Evaluation of Time Synchronization Precision

Time synchronization precision is evaluated by time synchronization considering the communication delay time mentioned in Section 2.4.3.

4.2.1. Experimental Methods

The integrated system used in the experiment consists of the following components: a navigation system (OS: Redhat 9.0, CPU 3.2 GHz, Memory: 2048 MB), in which time-synchronous server is operated; an intraoperative logging system (OS: Redhat 9.0, CPU 3.2 GHz, Memory: 2048 MB); a cancer identification system (OS: Windows XP, CPU: 3.2 GHz, Memory: 2048 MB); a positioning-information server (OS: Windows XP, CPU:3.2 GHz, Memory: 2048 MB); and an autofocusing robot (OS: Windows XP, CPU: 2.8 GHz, Memory: 512 MB). The communication condition is a 100 Mbase-T LAN environment. Each system performs transmission and reception depending on the communication conditions shown in Table 3.

Under the condition that only the navigation system be first connected to the integrated system, the intraoperative

Table 3. Communication condition (100 Mbase-T).

Agent	Communication data [byte]	Sampling Frequency [Hz]
(a)CancerDetection	1080	5
(b)AutoFocusingRobot	243	20
(c)Registration	942	10
(d)Navigation	1212	5
(e)Logging	2265	50

Table 4. Result of time synchronization (n=100).

Agent	Average of loop back time $(T2-T1)$ [msec]	Average of processing time (S) [msec]	Max loop back time [msec]
Logging	1.7±0.2	0.01	2.32
CancerDetection	0.59±0.13	0.03	1.69
AutoFocusingRobot	0.66±0.7	0.02	0.87
Registration	1.05±0.4	0.02	1.37

logging system, cancer identification system, positioning-information server, and autofocusing robot are connected to the platform sequentially turn to perform time synchronization with the intraoperative logging system.

4.2.2. Results of Experiments

As shown in **Table 4**, the time synchronization precision of each measurement system is within 2 ms and the maximum delay time is 2.3 ms.

4.3. Evaluation of Failure Tolerance of Time-Synchronous Server

We confirmed that if problems occur in the time-synchronous server, a substitute time-synchronous server is started and time consistency in the integrated system is maintained.

4.3.1. Experimental Methods

The integrated system used in the experiment consists of the following components: an autofocusing robot (OS: Windows, CPU 3.2 GHz, Memory: 2048 MB) (A); a cancer identification system (OS: Windows, CPU 3.04 GHz, Memory: 2048 MB) (B); a positioning-information server (OS: Windows, CPU 2.8 GHz, Memory: 512 MB) (C); and an intraoperative logging system (OS: Windows, CPU 1.04 GHz, Memory: 1024 MB). The system time of each system is recorded by the intraoperative logging system. The communication condition is a 100 Mbase-T LAN environment. Time-synchronous servers are mounted in (A), (B), and (C). Priorities of servers are set as (A)>(B)>(C). The time-synchronous server is first operated in (A).

Under the condition that systems (A), (B), and (C) are already connected to the integrated system, (A) and the time-synchronous server operating in (A) are disconnected from the integrated system. In a short time, (A)

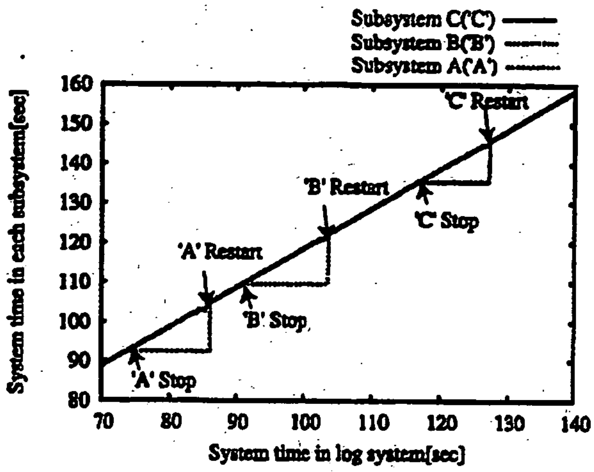

Fig. 6. Uniformity of time according to stop and restart of each timeserver.

is reconnected with the integrated system. We confirmed that even when (A) is reconnected, by synchronizing with the time-synchronous server (B), which started as a substitute for the (A), the time of (A) is made to match the time in the integrated system to maintain time consistency. For (B) and (C), it is performed under the same experimental conditions.

4.3.2. Results of Experiments

Figure 6 shows results of the measurement of time of each system accompanied by disconnection and reconnection of the system. The horizontal axis shows the system time for the intraoperative logging system and the vertical axis shows the integrated system time of systems (A), (B), and (C). As shown by **Fig. 6**, after disconnecting (A) from the integrated system, (A) is reconnected to the integrated system after an interval of several seconds. Compared to the time of (B) and (C), the time of (A) when reconnected has a time lag of 0 ms from (B) and 24 ms from (C), and integrated into the time in the integrated system without a lag of 30 ms or more. (A) performed time synchronization with the time server (B), which started as the substitute server for (A) in the integrated system. We confirmed that the time-synchronous server is correctly selected based on the specified priority.

Similarly, we confirmed that when disconnecting and reconnecting from the integrated system, the time of systems (B) and (C) is integrated with the time in the integrated system without a time lag of 30 ms or more.

4.4. Evaluation of Entire System by *in Vivo* Experiment

We confirmed basic navigation function under an environment simulating clinical use.

The integrated system is configured using five separately developed computer-assisted surgery systems (**Fig. 5**) (Section 3.1) communicating with each other. Communication interfacing of each system is defined as **Table 5**. Communication conditions are set as shown in

Table 5. Interface definition.

Agent	Communication interface
(a)CancerDetection	Property of cancer, measurement time
(b)AutoFocusingRobot	Robotic position, measurement time
(c)Registration	Setting position, measurement time
(d)Navigation	Integrated data(robotic position, setting position and property of cancer)
(e)Logging	All intraoperative data

Table 6. Computer specification.

Agent	RAM [MB]	CPU [MHz]	OS
(a)CancerDetection	512	2800	Windows XP
(b)AutoFocusingRobot	1024	3060	RedHat 9.0
(c)Registration	1024	3060	RedHat 9.0
(d)Navigation	1024	2400	FedoraCore 3.0
(e)Logging	2048	3060	Redhat 9.0

Table 3. Communication is done under the 100 Mbase-T LAN environment for the number of clients and (Table 3) communication data used in the integrated system, which ensures sufficient communication resources. Table 6 shows specifications for computers of computer-assisted surgical devices. Based on specifications in Table 6 and the policy under Results Section 4.1, time-synchronous server priority is set to (e), (c), (b), (d), and (a), in this sequence. Originally, data displayed in navigation is MRI images captured before surgery, but because preoperative image by MRI cannot be obtained in animal experiment facilities, dummy data is used, consisting of a porcine head imaged in advance.

4.4.1. Experimental Methods

An anesthetized pig (Landrace) is subjected to a craniotomy and 50 mg/kg of 5ALA, which is an excess quantity, is administered intravenously. In human subjects orally administered 5ALA, in the process of metabolism, 5ALA changes into PpIX, becoming fluorescent that accumulates selectively only in cancerous tissue. In our experiments, by intravenously administering greater amounts than those used in ordinary surgery, both cancerous and normal tissue uptakes the dye, 5ALA inducing PpIX, which accumulates and fluoresces from all exposed brain surfaces, where body movement of 5-10 mm is created at intervals of 6-7 seconds caused by the pig's breathing and heartbeat.

Based on such an *in vivo* test environment, we intentionally prepared nonfluorescent regions (Fig. 7(a) above), where the brain is covered by dura matter, protecting the brain surface, and fluorescent regions (Fig. 7(a) below), where the brain surface is exposed. Fig. 7(b) shows the brain surface exposed in reverse imaging and the unexposed region in normal imaging. Using autofocusing and scanning robots, scanning spans the boundary between fluorescent and nonfluorescent regions (Fig. 7) while maintaining a fixed distance between the instrument and object. Pp9 fluorescence is measured by a fluorescence detector having a spatial resolution of 0.6 mm.

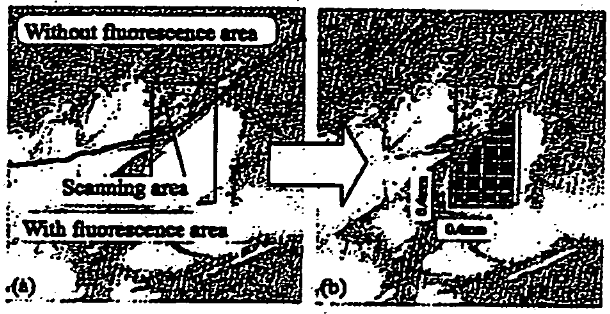

Fig. 7. Overview of brain surface with and without fluorescence area.

Table 7. Result of time synchronization (n=100).

Agent	Average of loop back time ($T2-T1$) [msec]	Average of processing time (S) [msec]
Logging	1.16±0.05	0.25
CancerDetection	0.7±0.28	0.21
AutoFocusingRobot	0.7±0.3	0.34
Registration	1.0±0.4	0.29

Specifically, a selected region is divided (Fig. 7(b)) into lattices at intervals of 0.4 mm, scanning stops on each lattice intersection and fluorescence is measured, then the next lattice point is moved to and measured. When fluorescence is measured, the spectral photometer is set to an exposure time of 200 ms. Fluorescence information (Fig. 7(b)) from cancer identification and information from the autofocusing robot showing the measurement position are integrated based on integrated time and displayed on the navigation screen as region information on fluorescent (red) and nonfluorescent (white) region.

4.4.2. Results of Experiments

Table 7 shows results of measurement of the time lag between the time-synchronous server of each system. Integrated system time is integrated with time-synchronous precision of 1 ms. After we conducted experiments for two hours, the time lag between the intra-operative measurement system and time-synchronous server was within 30 ms, i.e., it is 26 ms for the intra-operative measurement system (Windows) and 11 ms for the auto-focusing robot (Linux).

Figure 8 shows results of superposing the actual brain surface boundary of the region covered by dura matter (nonfluorescent) and that (fluorescent, reverse image) where the brain surface is exposed and the boundary (red: fluorescent, white: nonfluorescent) displayed on the navigation screen.

Unlike the MRI image of the pig, information measured during surgery is obtained as fluorescent by ensuring information integration based on the integrated time and displayed on the navigation screen having preoperatively photographed MRI image information, indicating that basic navigation functions are realized.

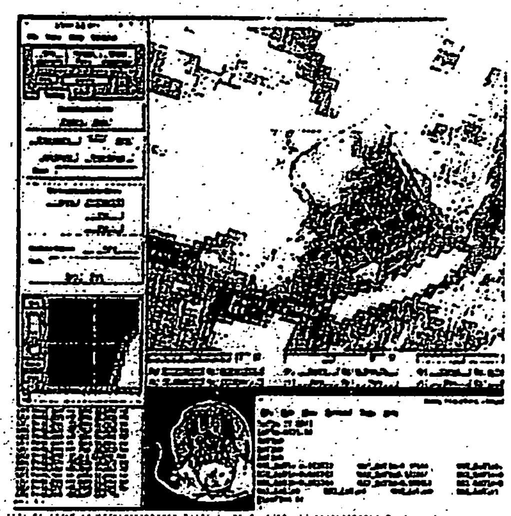

Fig. 8. Integration of Pp9 Spectrum data and 3D position data.

5. Discussion

5.1. Evaluation of Integrity of Integrated Time

Surgical information often is too sensitive, e.g., private patient information, to be sent via the Internet connection and NTP is often not available. When configuring a distributed system under such circumstances, a time lag exists between computer clock time and actual time. Given that integrated systems into surgery are continuously used for at least two to three hours, experiments indicate a time lag of about one second is created when using Windows.

As clarified by the result of the experiment, to realize time-synchronous precision of 30 ms required in our work, time synchronization must be within 8 minutes for Windows and 26 minutes for Linux. Since the clock fluctuates with Windows, we concluded that the frequency of the time-synchronous server must have a margin to realize time synchronization every 20 minutes for Linux and every 5 minutes for Windows.

5.2. Evaluation of Time Synchronization Precision

One may have an objection that if there is sufficient real time performance, when each time is different, there is no obstacle to function. Even if real-time performance of individual equipment software is ensured, it is unclear whether real-time performance is ensured for communication between equipment. Even if sufficient communication resources are ensured in the LAN when using the network, a communication lag of a maximum 40 ms may arise [7]. In the liver, for example, the positioning fluctuation of 50 to 60 mm may exist at intervals of 7 to 8 seconds. A time lag between measuring instruments could make treatment information unreliable when information is integrated. Our proposed time synchronization realizes precise time synchronization by considering communication time lags by measuring loop-back time with the time synchronization server. After determining network communication conditions, time is synchronized using Cristian's algorithm when a communication time lag is sufficiently short. Our experiments showed that time synchronization with precision of 2 ms is feasible.

5.3. Evaluation of Failure Tolerance of Time-Synchronous Server

Since sufficient time precision is maintained for short periods when switching to the clock in each computer, it could be assumed that fault-tolerant performance already existed.

Even when the time-synchronous server is disconnected, the time lag of each computer is considered small when system operating time is short. As discussed in Section 5.1.1, a time lag of 30 ms exists for 8 minutes for Windows. When considering that computer-assisted surgery is operates continuously for two to three hours, it becomes difficult to maintain time consistency in the integrated system without the time-synchronous server. As mentioned in Section 2.4.1, when a standard time-synchronous server is disconnected from the integrated system, consistency of information cannot be maintained.

The fault-tolerant time-synchronous server we propose copes with these problems because even if problems occur in the time-synchronous server, it continues to provide standard time in the integrated system.

5.4. Evaluation of Entire System by *in Vivo* Experiment

To reduce cost and development time when changing specifications and adding functions, we used distributed-object technology, developed communication components in which all functions such as time synchronization are involved, and applied these to a neurosurgery-assisted system.

An integrated navigation system is configured by integrating already developed computer-assisted surgical devices, but it takes almost a week. We have no choice but to evaluate development time with qualitative and subjective indexes because communication software is developed separately based on the environment is no longer required. Since time consistency is realized in the background by the communication component we developed, labor for developing the integrated system is reduced.

Through an *in vivo* evaluation experiment, we standardized time, which is important for integrating intra-operative information, using time-synchronous precision of 1 ms, equivalent to results of experiments in Section 4.2, i.e., 2 ms. The time lag is within 30 ms under continuous 2-hour system operation. Basic functions of integrated navigation are confirmed and that intra-operative measurement information from measurement systems such as cancer identification and the auto-focusing robot is integrated based on standardized time to be displayed on a navigation screen having preoperative diagnosis information.

Positron emission tomography/computed tomography (PET/CT) is an example ensuring multiple information integration. CT and PET are conducted on the same inspection bench, and by superposing both images, anatomical CT information is added to PET imaging. Cancer is located correctly, effectively improving the diagnostic yield.

We demonstrated the effectiveness of integrating multiple diagnostic information, although the integration of information is conducted only for the integration of preoperative image information. No system has, to our knowledge, been reported that integrates histological information such as brain malignancy by 5ALA induced Pp9 fluorescence measured during surgery, which our proposal realizes with anatomical and functional information obtained from diagnostic devices prior to surgery and shown in real time.

By proactively using both preoperative information and information from measurement equipment during surgery, the surgeon is encouraged to judge more exactly and effective treatment support is ensured. The integrated platform integrating intra-operative and preoperative information is expected to progress in the future as a basis for realizing more effective treatment support. To obtain precise treatment information, it is useful to realize and maintain precise time synchronization. We have shown that 30 ms time-synchronous precision is stably obtained under continuous two-hour system operation in an *in vivo* environment simulating clinical use, so more precise computer-assisted surgery is expected to be realized.

6. Conclusions

In our work, we have assumed a surgical environment in no Internet connection is available and have developed an integrated platform focusing on the integration of position and time. To realize such integration, we emphasized the importance of highly precise time standardization of subsystems and a redundant time-synchronous server.

We realized highly precise time integration by synchronizing time based on Cristian's algorithm under system environment limited to a LAN. Experiment confirmed highly precise time synchronization within 2 ms is realized.

We developed and implemented an algorithm in which a time-synchronous server is made redundant based on the number of surgical devices to be used, and integrated time information is maintained even when the time-synchronous server is not connected. In experiments evaluating performance, the standard time in the integrated system is not lost when the server is not connected and time consistency is maintained within a time-synchronous precision of 30 ms. Communication components combine communication and time-control components. Surgical navigation is configured using an integrated environment for neurosurgery and *in vivo* experiments confirmed basic navigation functions.

Acknowledgements

We thank the many people and groups who have contributed to this effort. Research on medical devices for analyzing, supporting, and substituting for the function of the human body was funded by the Ministry of Health, Labor, and Welfare of Japan.

References:

[1] K. Shimizu, S. Toyonori, E. Kobayashi, H. Inada, Y. Muragaki, T. Maruyama, H. Iseki, and I. Sakuma, "Application of blue semiconductor laser to measurement of 5-ALA induced fluorescence for intraoperative detection of brain tumor," Proceeding of 6th Japan-France Congress on Mechatronics and 4th Asia-Europe Congress on Mechatronics, pp. 135-140, 2003.

[2] M. Noguchi, E. Aoki, D. Yoshida, E. Kobayashi, S. Omori, Y. Muragaki, H. Iseki, K. Nakamura, and I. Sakuma, "A novel Robotic Laser Ablation System for Precision Neurosurgery with Intraoperative 5-ALA-induced PpIX Fluorescence Detection," In Proceedings of 7th International conference, MICCAI 2006, pp. 543-550, Copenhagen, Denmark, Oct., 2006.

[3] J. Hong, Y. Muragaki, T. Inomata, R. Nakamura, N. Hata, T. Dohi, and H. Iseki, "Intraoperative 3-D display of glioma for effective removal," JSCAS, pp. 235-236, Tokyo, Japan, 2004.

[4] E. Aoki, M. Noguchi, J. Hong, E. Kobayashi, R. Nakamura, T. Maruyama, Y. Muragaki, H. Iseki, and I. Sakuma, "Development and Evaluation of integrated surgical robotic platform for neurosurgery," JSCAS, pp. 89-90, Chiba, Japan, 2005.

[5] G. Coulouris, J. Dollimore, and T. Kindberg, "Distributed systems, Concepts and Design," Wokingham, Addison-Wesley, 3rd ed., 2001.

[6] P. Knappe, I. Gross, S. Pieck, J. Wahrburg, S. Kuenzler, and F. Kerschbaumer, "Position control of a surgical robot by a navigation system," Proceedings 2003 IEEE/RSJ International Conference on Intelligent Robots and Systems (IROS 2003), Vol.3, pp. 3350-3354, 2003.

[7] O. Schorr, N. Hata, A. Bzostek, R. Kumar, C. Burghart, R. H. Taylor, and R. Kikinis, "Distributed Modular Computer-Integrated Surgical Robotic Systems: Architecture for Intelligent Object Distribution," Medical Image Computing and Computer-Assisted Intervention (MICCAI), pp. 979-987, 2000.

[8] A. Bzostek, R. Kumar, N. Hata, O. Schorr, R. Kikinis, and R. H. Taylor, "Distributed Modular Computer-Integrated Surgical Robotic Systems: Implementation using modular software and network systems," Medical Image Computing and Computer-Assisted Intervention (MICCAI), pp. 969-978, 2000.

[9] S. Jia and K. Takase, "Internet-Based Robotic System Using CORBA as Communication Architecture," Journal of Intelligent and Robotic Systems, Vol.34, pp. 121-134, 2002.

[10] D. Levine and S. Mungee, "The Design and Performance of Real-Time Object Request Brokers," Computer Communications, Vol.21-4, 1998.

[11] G. Pardo-Castellote and S. Schneider, "The network data delivery service: real-time data connectivity for distributed control applications," Proceedings 1994 IEEE International Conference on Robotics and Automation, Vol.4, pp. 2870-2876, 1994.

[12] J. Tokuda, M. Hirano, T. Tsukamoto, T. Dohi, and N. Hata, "Real-Time Organ Motion Tracking and Fast Image Registration System for MRI-Guided Surgery," Systems and Computers in Japan, Vol.37, No.1, pp. 83-92, 2006.

[13] A. Pope, "The CORBA Reference Guide: Understanding the Common Object Request Broker Architecture," Englewood Cliffs, NJ, Prentice Hall, 1998.

[14] B. Dalton and K. Taylor, "Distributed Robotics over the Internet," IEEE Rob. Autom. Mag. 7(2), pp. 22-27, 2000.

[15] F. Cristian, "Probabilistic Clock Synchronization," Distributed Computing, Vol.3, pp. 146-158, 1989.

[16] http://www.slicer.org/

Name:
Eisuke Aoki

Affiliation:
Ph.D. student, Graduate School of Frontier Sciences, The University of Tokyo

Address:
7-3-1 Hongo, Bunkyo-ku, Tokyo 113-8656, Japan

Brief Biographical History:
2004 Master (Environmentology), Graduate School of Frontier Sciences, The University of Tokyo

Main Works:
• "System Design for Implementing Distributed Modular Architecture to Reliable Surgical Robotic System," Lecture Note in Computer Science 3217, pp. 184-191, 2004.

Membership in Academic Societies:
• The Japan Society of Computer Aided Surgery (JSCAS)
• The Robotics Society of Japan (RSJ)

Name:
Jae-Sung Hong

Affiliation:
Research Associate, Department of Nanobiomedicine, Faculty of Medical Sciences, Kyushu University

Address:
3-1-1 Maidashi, Higashi-ku, Fukuoka 812-8582, Japan

Brief Biographical History:
2004- JSPS Foreign Researcher, The University of Tokyo
2005- Research Associate, Kyushu University

Main Works:
• "An Ultrasound-driven Needle Insertion Robot for Percutaneous Cholecystostomy," Physics in Medicine and Biology, Vol.49(3), pp. 441-455, Jan. 2004.
• "Interventional Navigation for Abdominal Surgery by Simultaneous Use of MRI and Ultrasound," Medical and Biological Engineering and Computing, Vol.44(12), pp. 1127-1134, Dec. 2006.

Membership in Academic Societies:
• Japan Society of Computer Aided Surgery (JSCAS)

Name:
Masafumi Noguchi

Affiliation:
Ph.D. student, Graduate School of Frontier Sciences, The University of Tokyo

Address:
7-3-1 Hongo, Bunkyo-ku, Tokyo 113-8656, Japan

Brief Biographical History:
2005 Master (Environmentology), Graduate School of Frontier Sciences, The University of Tokyo

Main Works:
• "Development of a Compact Automatic Focusing System for a Neurosurgical Laser Instrument," Journal of JSCAS, Vol.6, No.4, pp. 483-489, 2004.

Membership in Academic Societies:
• The Japan Society of Computer Aided Surgery (JSCAS)

Name:
Etsuko Kobayashi

Affiliation:
Associate Professor, Department of Precision Engineering, School of Engineering, The University of Tokyo

Address:
7-3-1 Hongo, Bunkyo-ku, Tokyo 113-8656, Japan

Brief Biographical History:
2000- Research associate at the Univ. of Tokyo
2002- Lecturer at the Univ. of Tokyo
2006- Associate Professor at the Univ. of Tokyo

Main Works:
• "Development of Wide-Angle-View Laparoscope using Wedge Prisms," Journal of Robotics and Mechatronics, Vol.16, No.2, pp. 129-137, 2004.

Membership in Academic Societies:
• The Robotics Society of Japan (RSJ)
• Japan Society of Computer Aided Surgery (JSCAS)
• International Society for Computer Aided Surgery (ISCAS)

Name:
Ryoichi Nakamura

Affiliation:
Research Associate, Institute of Advanced Biomedical Engineering and Science, Tokyo Women's Medical University

Address:
8-1 Kawadacho, Shinjuku, Tokyo 162-8666, Japan

Brief Biographical History:
2001-2003 Visiting Researcher, Dept. of Radiology, Brigham and Women's Hospital and Harvard Medical School
2003- Research Associate, Tokyo Women's Medical University
2005- Research Assistant Professor, International Research and Educational Institute for Medical Science, TWMU

Main Works:
• "Control System for MR-Guided Cryotherapy – Short-term Prediction of Therapy Boundary Using Automatic Segmentation & 3D Optical Flow –," Lecture Note in Computer Science, 3217, pp. 542-550, June 2004.

Membership in Academic Societies:
• The Robotics Society of Japan (RSJ)
• International Society for Computer Aided Surgery (ISCAS)
• Japan Society of Computer Aided Surgery (JSCAS)

Name:
Takashi Maruyama

Affiliation:
Research Associate, Institute of Advanced Biomedical Engineering and Science, Tokyo Women's Medical University

Address:
8-1 Kawadacho, Shinjuku-ku, Tokyo 162-8666, Japan

Brief Biographical History:
1992- M.D., Faculty of Medicine, Showa University
1993- Research Fellow at Faculty of Neurosurgery, Graduate School, Tokyo Women's Medical University
1994- Research Fellow at Harvard Medical School, Brigham & Women's Hospital, Children's Hospital, Brain Tumor Research Center
1997- Ph.D. at Faculty of Neurosurgery, Graduate School, Tokyo Women's Medical University
1999- Board of Japan Neurological Surgery

Main Works:
• "Efficacy of 5-Aminolevulinic acid induced fluorescence detection in malignant glioma surgery," Springer, p. 1290, June 23-26, 2004.

Membership in Academic Societies:
• Japan Neurological Surgery

Name:
Yoshihiro Muragaki

Affiliation:
Assistant professor, Faculty of Advanced techno-surgery (FATS), Institute of advanced Biomedical Engineering & Science (ABME&S), Graduate school of Medicine (R&D), Tokyo Women's Medical University (TWMU) and Department of Neurosurgery, TWMU

Address:
8-1 Kawada-cho, Shinjuku-ku, Tokyo 162-8666, Japan

Brief Biographical History:
1986-1988 Resident of department of neurosurgery Tokyo Women's Medical College
1988- Attending staff of department of neurosurgery Tokyo Women's Medical College
1992- Board neurosurgeon of Japanese Neurosurgical Society
1992-1995 Visiting scientist of Department of pathology and laboratory Medicine of Pennsylvania University (USA; Prof. Trojanowski and Prof. Lee)
2000- Attending staff of Faculty of Advanced techno-surgery (FATS), Tokyo Women's Medical University
2006- Assistant professor of Faculty of Advanced techno-surgery (FATS) and Department of Neurosurgery, Tokyo Women's Medical University

Main Works:
• Y. Muragaki, T. T. Chou, D. R. Kaplan, J. Q. Trojanowski, and V. M. Y. Lee, "Nerve growth factor (NGF) induces apoptosis in human medulloblastoma cell lines that express TrkA receptors," Journal of Neuroscience, 17(2), p. 530.
• Y. Muragaki, H. Iseki, T. Maruyama, T. Kawamata, F. Yamane, R. Nakamura, O. Kubo, K. Takakura, and T. Hori, "Usefulness of Intraoperative Magnetic Resonance Imaging for Glioma Surgery," Acta Neurochirurgica Suppl., 98, pp. 67-75, 2006.
• Y. Muragaki, M. Hashizume, D. Hashimoto, H. Iseki, and K. Takakura, "A new concept of three-dimensional endoscope for practical use of endoscopic surgery," Surgical Endoscopy, (10), 2003, robotis and navigation system for advanced surgical procedures.

Membership in Academic Societies:
• The Japanese Society of Neurological Surgery
• The Japanese Society of Neuropathology
• The Japanese Computer Assisted Radiology and Surgery

Name:
Hiroshi Iseki

Affiliation:
Associate Professor, Faculty of advanced Techno-surgery, Institute of advanced Biomedical Engineering & Science, Graduate School of Medicine, Tokyo Women's Medical University

Address:
8-1 Kawada-cho, Shinjuku-ku, Tokyo 162-8666, Japan

Brief Biographical History:
1976- Research Assistant Professor at Dept. of Neurosurgery, Tokyo Women's Medical College (TWMC)
1996- Assistant Professor at TWMC
2001- Associate Professor at Tokyo Women's Medical University (TWMU)
2006- Professor at Tokyo Women's Medical University (TWMU)

Main Works:
• "Intelligent Operating Theater Using Intraoperative Open-MRI," Magnetic Resonance in Medical Sciences, 4(3), pp. 129-136, 2005.

Membership in Academic Societies:
• Japan Neurosurgical Society (JNS)
• Japan Society of Computer Aided Surgery (JCAS)
• Japan Society for Medical and Biological Engineering (JSMBE)

Name:
Ichiro Sakuma

Affiliation:
Professor, Department of Precision Engineering, School of Engineering, The University of Tokyo

Address:
7-3-1 Hongo, Bunkyo-ku, Tokyo 113-8656, Japan

Brief Biographical History:
1985-1987 Faculty of Engineering, The University of Tokyo
1987-1998 Faculty of Science and Engineering, Tokyo Denki University
1990-1991 Research Instructor at Baylor College of Medicine
1998-2001 Associate Professor at The University of Tokyo
2001- Full Professor at The University of Tokyo

Main Works:
• "Stem Cell Harvesting Device with Passive Flexible Drilling Unit for Bone Marrow Transplantation," IEEE Trans. Robotics Automation, 19, pp. 810-817, 2003.
• "A Dynamic Action Potential Model Analysis of Shock-Induced After effects in Ventricular Muscle by Reversible Breakdown of Cell Membrane," IEEE Trans. Biomed. Eng. 49, pp. 18-30, 2002.

Membership in Academic Societies:
• The Japan Society for Mechanical Engineers (JSME)
• Japan Society of Computer Aided Surgery (JSCAS)
• Japanese Society for Medical and Biological Engineering (JSMBE)
• The Japan Society for Precision Engineering (JSPE)
• The Institute of Electrical and Electronics Engineers (IEEE)
• International Society for Computer Aided Surgery (ISCAS)
• American Society for Artificial Internal Organs (ASAIO)
• Japanese Society for Electrocardiogram

生体医工学
45(2)：177-184, 2007

研究

MRIによる小型受信コイルの位置姿勢計測法の開発と評価

小野木真哉*・廖　洪恩**・渡部　滋***・小林英津子**・佐久間一郎**

Tracking Method of Small Receiver Coil Using MR Scanner

Shinya ONOGI,* Hongen LIAO,** Sigeru WATANABE,*** Etsuko KOBAYASHI,** Ichiro SAKUMA**

Abstract MR guided surgery is quite effective in realizing accurate and safe minimally invasive surgery (MIS). The combination of intra-operative MRI, surgical navigation system, and surgical robot should be of practical use in the field of MIS in the future. When we use flexible endoscope type robotic manipulator, the position and the orientation of the tip point of the flexible forceps should be navigated and controlled by a robotic manipulator. However, the conventional position sensor can not be used because of the strong magnetic field and the limited workspace. We propose a novel tracking method named extended active tracking (EAT), which is based on the active tracking algorithm. EAT can measure the position and the orientation of the tracking coils synchronically. The principle of EAT is three points measurement by three series inductance. We can calculate the orientation of three coils using the measured 3-D positions of coils. In this paper, three experiments was conducted to evaluate the basic performance of the EAT. First experiment is the flip angle adjustment for the reduction of background noise, which is caused by the proton around each inductance. The experimental results shown that the inductance positions could be clearly observed without background noise at 6-deg flip angle with NMR signal peaks. Second experiment is the reproducibility evaluation. The fluctuation of measurement position and orientation were less than 0.3 mm (SD) and 1.0 deg (SD) at various positions and orientations. And standard deviation of the distance between the inductances at various positions and orientations is less than resolution (0.78 mm). Third experiment is an accuracy evaluation. The position measurement accuracy was 0.39 mm (RMS) using an optical tracking device. The orientation measurement accuracy was 3.5 deg (RMS) when the tracking coil was rotated 30 degree. Evaluation result suggests that EAT is possible to be used inside a patient body with the required accuracy.

Keywords: Intra-operative MRI, MR guidance, device tracking.

1. はじめに

低侵襲手術に対する工学的支援としてコンピュータ外科がある．代表的なアプリケーションとしてはda Vinci (Intuitive Surgical Inc., California, USA) に代表される手術支援ロボットや，手術対象およびその周辺臓器等と術具の位置関係を二次元ないしは三次元のモデルで表示する手術ナビゲーションシステムなどがある．これらの利点を生かし，手術支援ロボットを術中画像誘導に用いることにより，安全かつ精密な治療が可能となる．そのなかでも，今後研究が進むと考えられるものとして，図1に示されるようなMRI下の軟性内視鏡下低侵襲手術システムが挙げられる．このシステムは術中MRI，手術ナビゲーションシステム，軟性鉗子，手術マニピュレータから構成される．術中画像誘導により患部の位置を正確に把握し，患部へのアプローチの自由度が高い軟性内視鏡型手術ロボットにより，患部に対して適切な治療を行おうとするものである[1-4]．

内視鏡下手術において，術具の位置・姿勢計測は不可欠である．特に手術ナビゲーションシステムを使用する場合はリアルタイムに術具の位置姿勢をトラッキングする必要があり，その計測結果を術前画像に重ねることで，術具と周辺臓器等との位置関係を提示する．また，手術ロボットの制御をするためにも術具先端の位置・姿勢を術中計測する必要がある．

現在，臨床の場で使用されている位置計測装置には，光を使用した光学式位置計測装置，磁場を利用した磁気式位

生体医工学シンポジウム2006発表（2006年，新潟）
2006年7月26日受付，2006年11月9日改訂，2006年12月7日再改訂，2007年1月11日再々改訂
Received July 26, 2006; revised November 9, 2006, January 11, 2007.
* 東京大学インテリジェントモデリングラボラトリー
Intelligent Modeling Laboratory, The University of Tokyo
** 東京大学大学院工学系研究科
Graduate School of Engineering, The University of Tokyo
*** 株式会社日立メディコ応用機器開発室
Application Development Office, Hitachi Medical Corporation

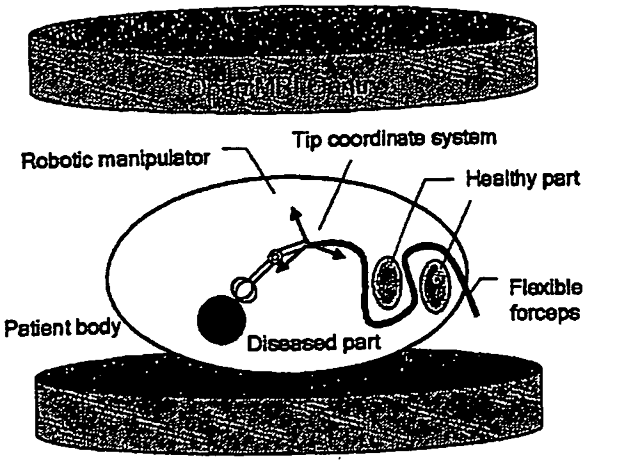

図1 オープンMRI下における軟性鉗子による低侵襲手術システムの構想

Fig. 1 System configuration of open-MRI guided minimally invasive surgery with flexible instruments.

置計測装置などがある．またMRI下に限定したものには傾斜磁場による位置計測法がある．これらの中で，MRI下で使用可能であるのは光学式および傾斜磁場方式である．光学式はケーブル等を必要とせずマーカーを計測対象に設置するのみで計測することが可能であるが，マーカーとセンサ（カメラ）の間で光が遮断されると計測できないという欠点がある．そのため，体内にある術具先端の位置・姿勢を直接計測することはできず，体外の術具根元の位置姿勢を計測し，順運動学を解くなどして術具先端位置を求める必要がある．従来の直線状鉗子型のロボット鉗子の位置・姿勢計測は，これが剛体であることから体外に置いた鉗子基部の位置を光学式位置計測装置で計測し，ロボットの関節角などの内部データから鉗子手先の位置・姿勢を計算することが可能であったが，軟性内視鏡型の能動鉗子の場合は動作によってその形状が時々刻々変化することから，鉗子先端の位置・姿勢を直接計測する必要がある．そのような用途に適したセンサとして，磁気式位置姿勢計測装置がある[5]．しかしながら磁気式センサはMRIの強力な磁場のもとでは使用不可能である．

MRI本体を利用した位置計測手法としては，傾斜磁場を利用する方法や小型受信コイル自体の位置を計測するアクティブトラッキングが報告されている．両者とも体内の特定点の位置を計測することができる．傾斜磁場による方式は，小型コイルで傾斜磁場の変化によって生じる誘導電流を計測することで，MRI下における位置と姿勢を計測するものである[6]．磁場を用いるため光学式にみられる光路遮断により計測が不可能になるといった事態はない．しかし，傾斜磁場の変化が小さい磁場中心付近では姿勢計測精度が悪いという報告がある[7]．磁場中心は画像が最も高コントラストで得られる場所であるため，その付近で計測精度が悪いことは大きな問題である．他の手法として，小型受信コイルを用いるアクティブトラッキングがある[8]．これは，小型受信コイルで位相エンコードを行わずに周波数エンコードのみで計測を行い，小型受信コイルの三次元位置を高速に測定する手法である．体内に小型受信コイルを挿入した状態で得られるプロジェクションデータはコイル近傍にのみ信号が得られる．すなわちピーク位置がコイルの一次元位置を示しており，XYZ各軸方向についてプロジェクションデータを得ることで，受信コイルの三次元位置を得ることができる．また，アクティブトラッキングは位相エンコードを行わずに一次元のプロジェクションデータから位置計測を行うため，繰り返し時間の3倍程度の時間で計測を行うことが可能である．この手法はカテーテル先端位置の誘導に応用されている[9-12]．一方，アクティブトラッキングは位置のみの計測であり姿勢を計測することはできないという課題がある．アクティブトラッキングを応用し，多点計測を可能とする方法の報告もなされている[13, 14]．Zhangら[13]は共振回路を二つ用意し，電磁誘導で二つの共振回路を一つの整合回路に接続している．デカップリングダイオードにアクティブに電流を流すことで，どちらの共振回路で計測を行うか選択することができるが，2点を同時に計測することはできない．そのため，2点を計測するためには2倍の時間（繰り返し時間×6）が必要となる．3軸周りの姿勢計測を行う場合は3点以上の計測が必要であるため，共振回路を3つ用意し，それぞれ計測する必要がある．その場合，計測時間が3倍となる（繰り返し時間×9）ことによる時間分解能の低下や回路の大きさが問題となる．例えば繰り返し時間を20 msecとした場合，3点の計測には180 msec必要となる．

Zhangら[14]は，直列分解したインダクタンスを直線状に配置し，2点の三次元位置から針やカテーテルなど直線状の器具に対し，先端の位置と角度を求める手法である．カテーテル先端位置は実際のコイル位置から幾何的に算出しているが，厳密には各コイルのどの位置においてピークが得られているか不明であるため，実際のカテーテル先端の位置姿勢と計測値との間に少なからず誤差を含むと考えられる．また，長軸周りの姿勢を計測できないため，術具先端位置を計測によりキャリブレーションを行うには情報が足りない．さらに，長軸周りの姿勢計測を行っていないことから，その姿勢が重要となる器具（メスや把持鉗子など）には適応できない．

これらの課題を踏まえ，本研究ではアクティブトラッキングを応用した6自由度全ての計測を実現する手法を考案した（拡張アクティブトラッキング，Extended Active Tracking，EAT）．本報告では3点の同時計測が行えることの確認をし，その基礎的評価として1)インダクタンス周辺の水によるノイズを軽減するためのフリップアングル調節，2)拡張アクティブトラッキングによる三次元位置姿勢計測再現性評価，3)拡張アクティブトラッキングによる三

次元位置姿勢計測精度評価を行ったので報告する．

2. 原理と実験装置

2·1 アクティブトラッキング法

アクティブトラッキングは小型受信コイル（トラッキングコイル）を用いた三次元位置計測法である．インダクタンスの感度はインダクタンス内部においてはよく，外部に対しては距離の二乗で低下する．そのため，大きなFOVに対して小型の受信コイルを用いて撮像すると，コイル近傍にのみ信号が得られる．そこで，位相エンコードを行わずに一次元計測を行うと，コイルの存在する位置にピークをもつプロジェクションデータが得られる．この計測をXYZ各軸に対して行うことで，高速にトラッキングコイルの三次元位置を計測することが可能である．

2·2 姿勢計測原理

3軸周りの姿勢計測を行うためには不等辺三角形を成す3点の三次元位置を計測できればよい．まず，三角形ABCを不等辺三角形とすることで三辺の長さが全て異なることから，計測された3点がそれぞれ点A，B，Cのどれかを同定することが可能である．三角形から独立な二つのベクトル*AB*と*AC*が得られる．例えば三角形ABCの座標系を，三角形の重心を原点，AB方向をX軸方向，三角形と同じ面内にY軸，三角形の法線方向をZ軸と定義する．i_xは*AB*の単位ベクトルである．i_zは*AB*×*AC*の単位ベクトルであり，i_yは$i_z \times i_x$である．よって，点A，B，Cの三次元位置からこの三角形の三次元位置と姿勢を求めることができる．

2·3 拡張アクティブトラッキングの原理

アクティブトラッキングを使用して同時に3点の位置計測を行うとすると，受信アンプが3台必要となり，汎用性に欠けるものとなる．3つのトラッキングコイルを切り替えて順次計測する場合は，同時ではないため計測中の移動による誤差や計測の時間分解能の低下が考えられる．そこで，受信コイルのインダクタンスを直列分解し，三角形と配置することで，受信アンプ1台で3点の三次元位置を同時に計測することができ，従来の位置姿勢計測装置と同様の位置姿勢計測が可能な手法を考案した．原理を図2に示す．分割された各インダクタンスはそれぞれの近傍に狭い感度領域をもつことから，各インダクタンスの位置にピークをもつプロジェクションデータが得られる．これは一次元上の各インダクタンスの位置を示すから，この計測を各軸方向に対して行うことで，各インダクタンスの三次元位置を計測することが可能である．

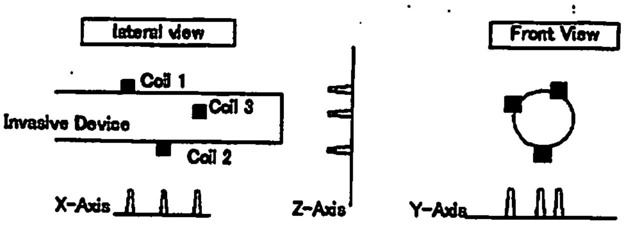

図2　拡張アクティブトラッキングの原理．プロジェクションデータのピーク位置から各インダクタンスの一次元位置がわかる．3点の三次元位置から受信コイルの三次元位置と姿勢を計算することができる

Fig. 2　The principal of extended active tracking method. The one-dimensional projection data indicates the position of each inductance. The position and orientation of device is calculated from the spatial positions of the three inductances.

2·4 MRIスキャナ

MRIには実験用に試作した0.2 Tオープン型MRIを使用した．上下に永久磁石があり，そのギャップは30 cmである．磁場強度が0.2 Tであることから，水素原子核のLarmor周波数は8.5 MHzとなる．

2·5 トラッキングコイル

開発した位置・姿勢計測用小型受信コイル（トラッキングコイル）は共振回路・整合回路・同軸ケーブルから成る（図3）．共振回路の共振周波数は8.5 MHzであり，インダクタンス成分は3つに直列分解されている．各インダクタンスは中空の樹脂に20回巻かれており，樹脂内部に信号源として水を封入した．このトラッキングコイルによるMRI画像・プロジェクションデータを図4に示す．このように，各インダクタンス内部の水から信号が得られており，プロジェクションデータにおいても各インダクタンスの位置においてピークが得られた．

2·6 信号処理方法

計測された各軸方向のプロジェクションデータからピーク位置を抽出した．ピーク位置には上位3点の極大値の位置を3つのピークそれぞれとして採用した．

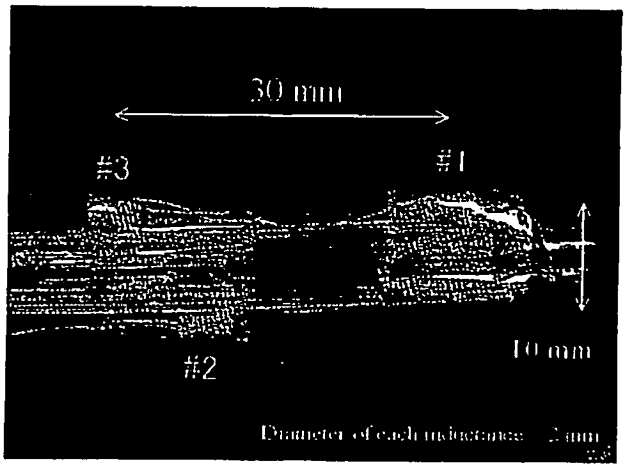

図3　作成したトラッキングコイルの外観．各インダクタンスは中空の樹脂に巻かれており，内部には信号源として水を封入している

Fig. 3　The manufactured receiver coils. Each inductance is wound around a water-filled plastic cylinder hollow.

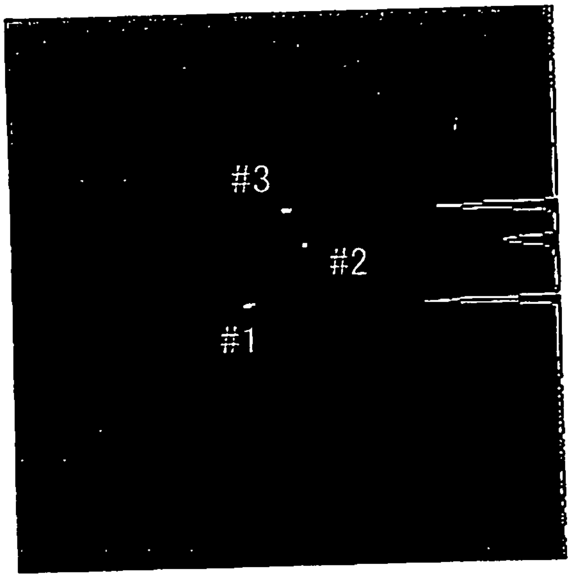

図4　作成したトラッキングコイルによるMRI画像とプロジェクションデータ
Fig. 4　MR image and projection data achieved by the tracking coils.

ピーク位置から各インダクタンスの三次元位置への同定方法について説明する．まず，予め2次元のMRI画像から各インダクタンス間の距離を求めリファレンスとした．計測したピーク位置（3点×3軸）を総当りで各インダクタンス位置とし，各インダクタンス間距離とリファレンスにおけるインダクタンス間距離の二乗誤差の和が最も小さくなる値を正しいコイルの組み合わせとした．

求めた各インダクタンスの三次元位置からトラッキングコイルの位置姿勢の算出に関しては，重心をトラッキングコイルの位置とし，2·2節で述べた手法でトラッキングコイルの姿勢を求めた．

3. 評 価 方 法

全ての実験において，パルスシーケンスはグラディエントエコー法を使用した．撮像パラメータはTR=40 msec, TE=12 msec，FOV=200 mmとした．位置計測の分解能は周波数エンコードの分解能256とFOV=200 mmから0.78 mmである．

3·1　ノイズ軽減のためのフリップアングルの調節

インダクタンス内部に信号源を用意したことで，インダクタンス周辺に信号源が無くとも位置計測を可能とした．一方，周辺に臓器等がある場合，そこからの信号が原因で明確なピークが得られない可能性がある．そこで，フリップアングルを調節することで周辺の水素による影響を軽減する手法を検討した．実験はコイルを防水した上，水の入った容器にコイルを設置した状態で行った．フリップアングルを30度から3度刻みで3度まで変化させた．S/N比を（3つのピークの最小値）/（周辺の水による信号の最大値）と定義し，各フリップアングルとS/N比について評価した．

3·2　位置・姿勢計測再現性評価

同じ位置にインダクタンスを設置した場合の計測結果の変動を評価した．トラッキングコイルを固定した状態で20回連続して位置・姿勢計測を行い，三次元位置の標準偏差，各方向ベクトルの角度の標準偏差を求めた．上記20回計測による評価を6種類の位置・姿勢において行い，FOV中の位置によって再現性に違いがないか確認した．

またトラッキングコイルの位置姿勢によって各インダクタンス間の距離，すなわちインダクタンスの成す三角形の形状が一定であるか確認した．10種類の位置・姿勢に対して，各インダクタンス間の距離の揺らぎを評価した．

3·3　計測精度評価

本手法による計測精度（正確さ）の評価を行った．位置計測精度は，トラッキングコイルと赤外線マーカーを樹脂製の板に固定し，平行移動した移動距離を本手法と光学式位置計測装置（Polaris, NDI, Canada）の計測結果から比較・評価した（図5）．平行移動させた方向は任意の方向とし，XYZ全ての軸方向に移動が生じるようにした．姿勢計測精度評価は，30度間隔で回転させることが可能な樹脂製の器具を製作し，任意の軸回りに初期位置から30度刻みで180度まで回転を行うことで器具の回転角と計測値を評価した（図6，図7）．回転角度は回転前と回転後の間の変換行列を求め，その変換行列Tから，i行j列目の要素をT_{ij}のように表すと

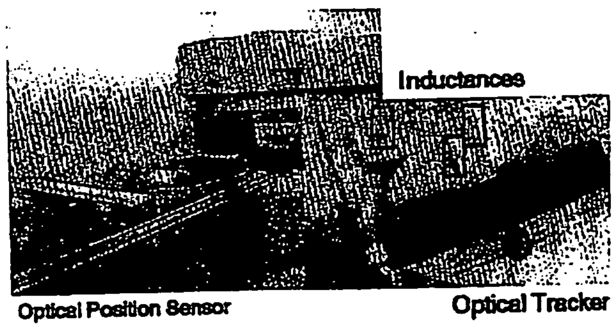

図5　光学式計測装置と本手法による精度評価実験環境
Fig. 5　Experimental settings of the position accuracy evalua tion for EAT method and optical tracking method.

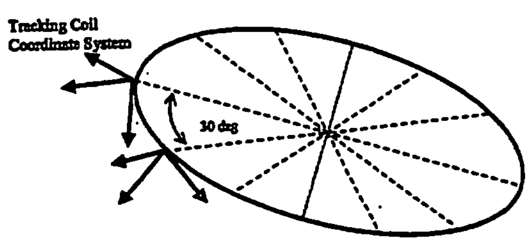

図6　姿勢計測実験の模式図．トラッキングコイルを任意の 周りに30度回転させ評価した
Fig. 6　Experimental settings of the orientation accura evaluation. The tracking coil is rotated 30-degr around an optional axis.